

Magnetic phase diagram of a partially frustrated triangular antiferromagnet: The row model

M. E. Zhitomirsky*

L. D. Landau Institute for Theoretical Physics, Moscow 117334, Russia

(Received 17 October 1995; revised manuscript received 22 January 1996)

Phase diagram of a planar antiferromagnet on a stacked triangular lattice subject to a uniform orthorhombic distortion is studied within the Landau approach. This spin system with partially released frustration exhibits a variety of ordered phases in magnetic field parallel to the basal plane including elliptically and linearly polarized incommensurate structures. Four magnetically ordered phases coexist at a multicritical point. The theory is applied to explain the experimental phase diagram of RbMnBr_3 and satisfactory agreement for temperature dependences of critical fields is found. [S0163-1829(96)03526-6]

I. INTRODUCTION

Magnetic ordering phenomena in spin systems with geometrical frustration are a subject of numerous studies. The simplest model of this type is the Heisenberg antiferromagnet on a triangular lattice, which has the noncollinear 120° spin structure as the ground state. An interesting example of partial lifting of frustration on triangular lattice has been found among ABX_3 -type hexagonal antiferromagnets. A number of compounds from this family undergoes structural transitions in their stacked triangular lattice of magnetic ions before spin ordering occurs.¹ This leads to distortion of some spin bonds and partially released frustration on an elementary triangular plaquette. One of the intriguing possibilities addressed in this connection is the splitting of ordering transition for chiral and continuous degrees of freedom under appropriate lattice distortion.² Theoretical studies of such antiferromagnets reveal also many new otherwise unstable spin phases both in a zero²⁻⁵ and in a finite⁶ field.

Magnetic properties of RbMnBr_3 are the most complicated among other triangular antiferromagnets with partially released frustration. Earlier neutron diffraction measurements⁷ have found an incommensurate helical spin structure with a turn angle different from 120° at zero field. An additional low-field transition for magnetic fields directed within the basal plane, not observed in the fully frustrated compound CsMnBr_3 ,⁸ has been detected in RbMnBr_3 by an anomaly in the magnetization curve⁹ and by a surprising behavior of the lowest branch of resonance spectrum.¹⁰ Further neutron scattering experiments¹¹⁻¹³ confirmed this transition and resolved more complicated structure of Bragg reflections which include two triads of magnetic peaks near to $(1/3, 1/3, 1)$ at $H=0$.¹² Comparison of magnetization and neutron data obtained on different samples provides strong support in favor of a multicritical point in the magnetic diagram of RbMnBr_3 at which four different spin phases coexist (see Fig. 1).¹⁴ Two of these phases, I and II, were identified as having the same incommensurate ordering wave vector.¹² Suggestion of the multicritical point is also supported by the measurement of all phase boundaries on a single sample.¹⁵

Incommensurate spin helix in RbMnBr_3 at zero field has been attributed by a number of authors^{3,4} to a small uniform orthorhombic distortion of the underlying hexagonal lattice which yields two nonequivalent exchange bonds in the basal

plane: inside horizontal rows and in between as shown in Fig. 2. It was shown later that the row model also explains the low-field transition at $T=0$ as a lock-in transition from the incommensurate spin helix to the commensurate 120° structure.⁶

This simple assumption about the symmetry of the lattice of RbMnBr_3 at low temperatures confirmed by the birefringence measurements of Kato *et al.*¹⁶ was questioned in the interpretation of neutron data.¹² In addition, a model involving an exotic three-site biquadratic exchange has been recently proposed as an alternative explanation of the spin structure.¹⁷ Existence of such interactions in RbMnBr_3 is, however, quite doubtful. The conclusion of Ref. 17 that the magnetic scattering data¹² can only be explained by the model parameters corresponding to the phase boundary between different states also reduces probability of this scenario.

Recent neutron scattering measurements¹⁸ performed on a sister compound KNiCl_3 , which has an analogous sequence

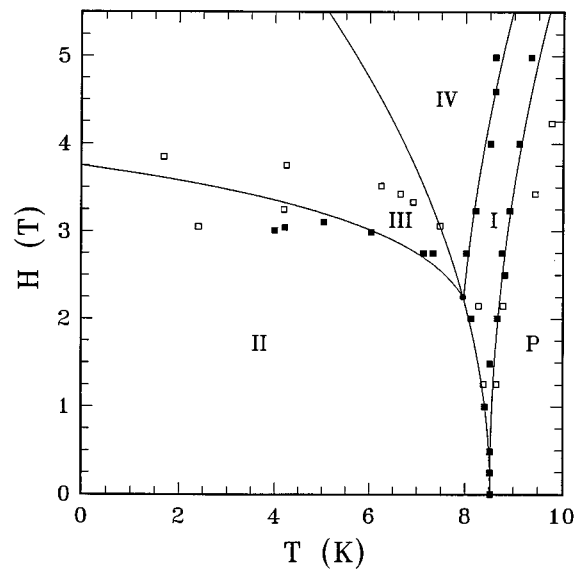


FIG. 1. The phase diagram of RbMnBr_3 for magnetic fields lying in the basal plane. Open and solid squares are experimental data from Refs. 9 and 12, respectively; solid lines are theoretical curves. The paramagnetic phase is denoted by P .

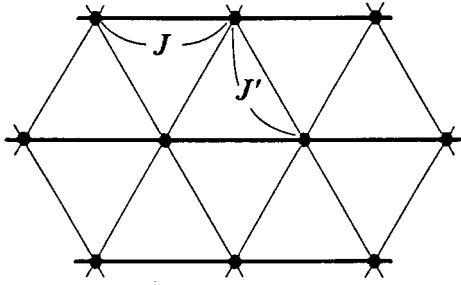


FIG. 2. Schematic structure of in-plane spin bonds in the row model.

of structural transitions,¹⁹ show the same triad of magnetic peaks around $(1/3, 1/3, 1)$ at $H=0$ as in the high-field phase IV. Since additional transitions in magnetic field are absent for KNiCl_3 , this observation proves that the details of the magnetic order as seen from Bragg patterns¹² are not crucial for both the appearance of incommensurate spin spiral and the unique phase diagram of RbMnBr_3 .

In order to verify which type of spin bond deformation is responsible for the experimental multiphase diagram, we study in this paper the whole H - T diagram of the row model using the phenomenological Landau-type theory. This approach gives qualitatively the same phase diagram as observed for RbMnBr_3 . Four different ordered phases of the row model are combined in Fig. 3. They include two linearly polarized phases and two phases with elliptic polarization, one phase in each pair being incommensurate and the other commensurate. Furthermore, the correct temperature dependences of critical fields in the vicinity of the Néel temperature T_N are recovered in our treatment.

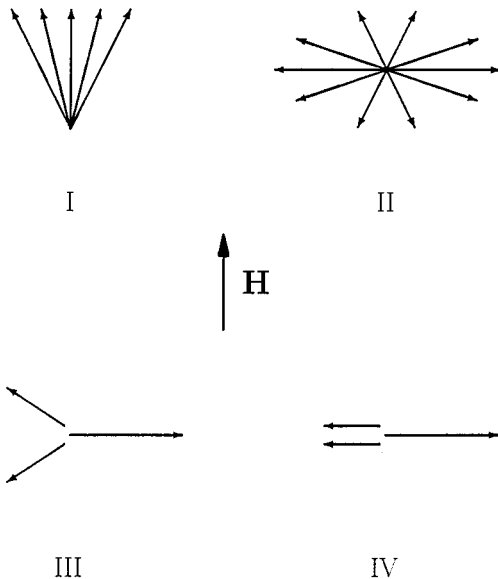


FIG. 3. Four magnetically ordered phases of the row model in magnetic field. Arrows represent spins for the phase I and antiferromagnetic vectors of adjacent chains in the other cases.

II. MODEL

The Hamiltonian of the XY spin model on a stacked triangular lattice subject to a orthorhombic distortion is given by

$$\hat{\mathcal{H}} = J_{\parallel} \sum_{\langle i,j \rangle} \mathbf{S}_i \cdot \mathbf{S}_j + J \sum_{\langle k,l \rangle} \mathbf{S}_k \cdot \mathbf{S}_l + J' \sum_{\langle m,n \rangle} \mathbf{S}_m \cdot \mathbf{S}_n - \sum_i \mathbf{H} \cdot \mathbf{S}_i, \quad (1)$$

J_{\parallel} is the interplane exchange coupling, and bonds corresponding to J and J' are shown in Fig. 2. All exchange constants are antiferromagnetic for RbMnBr_3 . The ground state of the system at $H=0$ is a spin helix

$$\mathbf{S}_n = \text{Re}[\text{Sexp}(i\mathbf{k} \cdot \mathbf{r}_n)] = l_1 \cos(\mathbf{k} \cdot \mathbf{r}_n) + l_2 \sin(\mathbf{k} \cdot \mathbf{r}_n). \quad (2)$$

For undistorted hexagonal lattice ($J=J'$) spins form the commensurate triangular structure described by the wave vector $\mathbf{Q} = (4\pi/3, 0, \pi)$ and circular polarization of the complex amplitude $\mathbf{S} = l_1 + il_2$: $|l_1| = |l_2|$, $l_1 \perp l_2$. Adjacent spins on different planes are antiparallel in this structure, while at the same plane they are directed at 120° to each other.

An orthorhombic deformation of the lattice shown in Fig. 2 partially lifts frustration on an elementary plaquette and 120° configuration of spins becomes unstable. Minimizing exchange energy in (1) with respect to the wave vector \mathbf{k} , one finds at $H=0$:

$$\cos k_x/2 = -J'/2J. \quad (3)$$

Thus, the ground state is an incommensurate spin helix propagating in the direction of rows. If, however, the relative difference of two in-plane exchange constants $\delta = (J'/J - 1)$ is small, the spin configuration has locally triangular structure with the vector pair (l_1, l_2) rotating uniformly from point to point by the angle $\varphi = \mathbf{q} \cdot \mathbf{r}$, $\mathbf{q} = [(2/\sqrt{3})\delta, 0, 0]$. In the continuum limit this modulation of the 120° spin structure appears due to the Lifshitz invariant compatible with the reduced symmetry of the lattice.⁶

$$-\frac{\sqrt{3}}{2} J \delta S^2 \frac{d\varphi}{dx}. \quad (4)$$

III. LANDAU THEORY

We use the Landau-type approach in our study of the phase diagram of the model (1). This mean-field approach is qualitatively correct for spin systems in three dimensions. In fact, the Monte Carlo simulations for temperature dependences of critical fields of fully frustrated model ($J'=J$) gave a very small deviation from the square-root law obtained in the Landau-type theory.²⁰ Such phenomenological symmetry consideration was successfully used earlier to explain magnetic phase diagrams of the easy-axis and the easy-plane antiferromagnets CsNiCl_3 and CsMnBr_3 ,^{21,22} which have perfect stacked triangular lattices.

A. Free-energy functional

We begin derivation of the free-energy functional with the case of a fully frustrated triangular antiferromagnet. The complex Fourier amplitude \mathbf{S} in Eq. (2) fulfills the role of the order parameter for this system. Its modulus becomes non-

zero at $T < T_N$, while magnetic field changes the type of polarization. The free-energy density F is a function of \mathbf{S} , which should be invariant with respect to spin rotations, lattice translations [$\mathbf{S} \rightarrow \mathbf{S} \exp(i\pi/3)$], and lattice rotations ($\mathbf{S} \rightarrow \mathbf{S}^*$). An expansion of F in powers of the order parameter yields

$$F = \alpha(T - T_N)(\mathbf{S}^* \cdot \mathbf{S}) + \beta_1(\mathbf{S}^* \cdot \mathbf{S})^2 + \beta_2|\mathbf{S} \cdot \mathbf{S}|^2 + \chi_1 H^2(\mathbf{S}^* \cdot \mathbf{S}) + \chi_2 |\mathbf{H} \cdot \mathbf{S}|^2 - \frac{1}{2} \gamma [(\mathbf{S} \cdot \mathbf{S})^3 + \text{c.c.}]. \quad (5)$$

In contrast to the previous analyses,^{21,22} we have excluded from the free-energy functional uniform magnetization, which is a noncritical mode, and write instead invariants of the order parameter with the magnetic field. The sixth-order term included in (5) was introduced by Zhu and Walker.²¹ It serves to lift the remaining degeneracy of the order parameter in cases specified below. Note, that the form of this invariant is determined by the relation $6\mathbf{Q} = \mathbf{G}$, \mathbf{G} being a reciprocal lattice vector. Other possible sixth-order terms are unimportant for our purpose, since they only renormalize critical fields [as, e.g., $(\mathbf{S} \cdot \mathbf{S}^*)^3$] or yield a zero-field anisotropy in the basal plane,²¹ which is absent on experiment.

The type of the spin ordering at zero field is determined by the second fourth-order term in (5), which one should take with a positive coefficient $\beta_2 > 0$ to reproduce the helical polarization of the spin wave (2).

Let us consider now modifications to the Landau functional (5) which are connected with the lower symmetry of the crystal lattice in the row model. If the distortion of exchange bonds is small, the ground state corresponds to an incommensurate spin helix with a wave vector slightly different from \mathbf{Q} . This assumption is apparently applied to RbMnBr₃, as its helix angle was estimated to be about 128°. ^{7,12} In this case the continuum approximation can be used, which treats the difference between the real wave vector and the vector \mathbf{Q} as an extra slow space modulation of the order parameter $\mathbf{S}(\mathbf{r})$. An instability of the commensurate triangular structure is described in this approximation by the following Lifshitz invariant:

$$\frac{1}{2} B i (\mathbf{S}^* \cdot \partial_x \mathbf{S} - \mathbf{S} \cdot \partial_x \mathbf{S}^*),$$

where the phenomenological constant B is given in the classical limit by (4). The presence of such an invariant is explained by breaking of a small symmetry group of the ordering wave vector from C_3 to C_1 under orthorhombic deformation of the hexagonal lattice. To ensure stability of the system, the Lifshitz invariant should be combined with the usual spin rigidity term quadratic in gradients: $A |\partial_x \mathbf{S}|^2$, $A > 0$. Finally, we obtain the following energy functional appropriate to study phase transformations of the row model

$$F = \alpha(T - T_N)(l_1^2 + l_2^2) + \beta_1(l_1^2 + l_2^2)^2 + \beta_2[(l_1^2 - l_2^2)^2 + 4(\mathbf{l}_1 \cdot \mathbf{l}_2)^2] + \chi_1 H^2(l_1^2 + l_2^2) + \chi_2 [(\mathbf{H} \cdot \mathbf{l}_1)^2 + (\mathbf{H} \cdot \mathbf{l}_2)^2] + A[(\partial_x l_1)^2 + (\partial_x l_2)^2] + B(\mathbf{l}_1 \cdot \partial_x l_2 - \mathbf{l}_2 \cdot \partial_x l_1) - \frac{1}{2} \gamma \{[(\mathbf{l}_1 + i\mathbf{l}_2)^2]^3 + \text{c.c.}\}. \quad (6)$$

Signs of different phenomenological constants, $\beta_2 > 0$, $\chi_1 < 0$, $\chi_2 > 0$, $\gamma > 0$, we chose the same as for fully frustrated triangular antiferromagnet CsMnBr₃.²² The zero-field phase of (6) is a modulated triangular spin structure $\mathbf{S} \propto (\hat{\mathbf{e}}_1 + i\hat{\mathbf{e}}_2) \exp[-i\varphi(\mathbf{r})]$, where $\hat{\mathbf{e}}_1$ and $\hat{\mathbf{e}}_2$ are two perpendicular unit vectors in the basal plane and $\varphi(\mathbf{r}) = (B/2A)x$. The smallness of the phase variation between two adjacent sites $(B/2A) \ll 1$ is necessary to justify a validity of the continuum approximation. Accordingly, we neglect a small shift of the Néel temperature on $\delta T_{ic} = B^2/4\alpha A$ resulting from such long-wave modulations. Note that T_N does not split for this type of bond deformation.

B. Linearly polarized phases

In this subsection we consider a sequence of transitions which occurs in high magnetic fields (between phases P and I and phases I and IV in Fig. 1). Basal plane magnetic field creates anisotropy for spins described by $\chi_2 |\mathbf{H} \cdot \mathbf{S}|^2$. This term favors linear polarization of \mathbf{S} with polarization vector directed perpendicular to the field for $\chi_2 > 0$. Choosing $\hat{\mathbf{e}}_1 \perp \mathbf{H}$, we have at high fields the order parameter of the form $\mathbf{S} = l \hat{\mathbf{e}}_1 \exp(-i\varphi)$ with the free-energy density written as

$$F = \alpha(T - T_N)l^2 + \chi_1 H^2 l^2 + \beta_{12} l^4 + A(\partial_x l)^2 + A l^2 (\partial_x \varphi)^2 - B l^2 (\partial_x \varphi) - \gamma l^6 \cos 6\varphi, \quad (7)$$

where $\beta_{12} = \beta_1 + \beta_2$. Energy functionals of such a form are typical for weakly incommensurate systems.^{24,25} Equations on the order parameter obtained by minimizing Eq. (7) with respect to l and φ cannot be solved analytically. In our case, however, the anisotropy term, which favors commensurate states, is of the sixth order in l , i.e., near T_N it has an additional smallness compared to other homogeneous terms. Therefore, we can use a so-called constant amplitude approximation.^{24,25} Its simplifying assumption is that the amplitude l is constant in space and should be found from the first three terms in (7), while the space varying phase $\varphi(x)$ is determined by the last three terms.

The factor before l^2 changes sign at the critical field

$$H_N(T) = [\alpha(T - T_N)/|\chi_1|]^{1/2}, \quad (8)$$

after which the amplitude l is finite:

$$l^2 = [\alpha(T_N - T) + |\chi_1| H^2] / 2\beta_{12}. \quad (9)$$

Here we have assumed that $\chi_1 < 0$ in accordance with the experiment. In the vicinity of the critical line $H_N(T)$, the six-order anisotropy is small compared to gradient terms and $\varphi(x) = (B/2A)x$. The order parameter in phase I is linearly polarized perpendicular to \mathbf{H} , while spins form an incommensurate fan structure oscillating in a finite angle around \mathbf{H} . As temperature decreases from $T_N(H)$, the spatial varia-

tion of $\varphi(x)$ in state I becomes more complicated due to increasing anisotropy and is described by the elliptic amplitude.²⁴ Near the I-IV phase boundary $\varphi(x)$ is locked to a set of commensurate values $\varphi_n = (1/3)\pi n$ (for $\gamma > 0$) in wide regions of space separated by thin domain walls or solitons. Interaction between walls is exponentially small and repulsive at large distances. Therefore, the incommensurate-commensurate transition can be studied within a single soliton picture. For a functional of the general form

$$F = X(\partial_x \varphi)^2 - Y(\partial_x \varphi) - Z \cos 6\varphi,$$

a single domain wall situated at $x=0$ is given by

$$\varphi_0(x) = \frac{2}{3} \arctan[\exp(2Zx/X)].$$

Its energy

$$E_{\text{DW}} = \frac{4}{3} \sqrt{2XZ} - \frac{1}{3} \pi Y$$

vanishes indicating an instability of the commensurate state for the following critical relation of parameters:

$$XZ/Y^2 = \pi^2/32. \quad (10)$$

Substituting expressions for X , Y , and Z from (7) into (10) we find the transition field between phases I and IV:

$$H_{\text{I-IV}}(T) = \left[\frac{\alpha(T + \delta T - T_N)}{|\chi_1|} \right]^{1/2},$$

$$\delta T = \frac{\pi B \beta_{12}}{\sqrt{8A \gamma \alpha}}. \quad (11)$$

The amplitude l is given in both phases by the same formula (9).

The linearly polarized commensurate phase IV with $l_1 \neq 0$, $l_2 = 0$ was identified as a high-field phase of the planar antiferromagnet CsMnBr₃.^{22,23} The temperature shift δT of the lock-in transition from $T_N(H)$ is much larger than the neglected renormalization of the Néel temperature δT_{ic} , which is quadratic in B . To avoid misunderstanding, we emphasize that the sixth-order term $[(\mathbf{S} \cdot \mathbf{S})^3 + \text{c.c.}]$ in (5) and the resulting anisotropy in (7) derived previously for the commensurate spin-wave are nonvanishing in the incommensurate state I, because at $H \neq H_N(T)$ this state corresponds to a multi- \mathbf{k} structure with the admixed commensurate harmonic.²⁴

In the used approximation the phase transition between incommensurate and commensurate states is continuous with standard logarithmic singularities for various physical quantities.²⁴ On the other hand, experiments indicate a discontinuous first-order transition in RbMnBr₃.⁹⁻¹² This discrepancy can be explained by going beyond the constant amplitude approximation. If the amplitude l is allowed to vary in space, a qualitatively new oscillatory behavior of l and φ far from domain wall is found in a certain range of parameters.²⁶ As a consequence, the asymptotic interaction of two solitons can be repulsive or attractive depending on the distance between them. The system will then prefer a discontinuous transition from the commensurate phase to a

soliton lattice. According to Ref. 26, the oscillatory behavior of l and φ occurs if the lock-in transition is close enough to $T_N(H)$:

$$\delta T < \delta T_{\text{cr}} = (B^2/2\alpha A) \left(\frac{3}{4} \pi + 1 \right)^2 \approx 23 \delta T_{\text{ic}}. \quad (12)$$

Because of the large prefactor in (12), one can have $\delta T_{\text{ic}} \ll \delta T \leq \delta T_{\text{cr}}$. This means that the transition to the commensurate state is only weakly first order and the critical temperature can still be calculated by using the single soliton picture (10).

C. Elliptically polarized phases

The linear polarization of the order parameter is energetically unfavorable at low fields where the fourth-order term $|\mathbf{S} \cdot \mathbf{S}|^2$ becomes important. The elliptic states II and III correspond to the following order parameter:

$$\mathbf{S} = (l \hat{\mathbf{e}}_1 + im \hat{\mathbf{e}}_2) \exp[-i\varphi(\mathbf{r})], \quad (13)$$

with space varying and constant phase φ , respectively. The commensurate phase III is the low-field state of the fully frustrated model.^{22,23}

Following the constant amplitude approximation we substitute the order parameter (13) into the energy functional (6) and neglect gradients of l and m . Transition to an elliptic phase is determined by the homogeneous second- and fourth-order terms

$$F' = \alpha(T - T_N)(l^2 + m^2) + \beta_1(l^2 + m^2)^2 + \beta_2(l^2 - m^2)^2$$

$$+ \chi_1 H^2(l^2 + m^2) + \chi_2 H^2 m^2, \quad (14)$$

which are independent of the phase φ . Therefore, phase boundaries between two incommensurate states I and II and two commensurate states III and IV are given in this approximation by the same formula

$$H_c(T) = \left[\frac{\alpha(T_N - T)}{\chi_3} \right]^{1/2}, \quad \chi_3 = \frac{\beta_{12}}{2\beta_2} \chi_2 - |\chi_1|. \quad (15)$$

After the second-order transition at $H = H_c$, the amplitudes l and m are

$$l^2 = m^2 + \frac{\chi_2 H^2}{4\beta_2}, \quad m^2 = \frac{\chi_3}{4\beta_1} (H_c^2 - H^2). \quad (16)$$

The curve $H_c(T)$ crosses with the phase boundary $H_{\text{I-IV}}(T)$ at some point in the H - T phase diagram. We show now that an additional line of phase transitions between the elliptic states II and III emerges from the same point.

Neglecting spatial variations of the amplitudes l and m , the gradient and anisotropy energies for the order parameter (13) are expressed as

$$F'' = A(l^2 + m^2)(\partial_x \varphi)^2 - B(l^2 + m^2)(\partial_x \varphi)$$

$$- \gamma(l^2 - m^2)^3 \cos 6\varphi. \quad (17)$$

Making use of (16), one gets for the anisotropy of the elliptic phase in magnetic field $E_{\text{an}} \propto -H^6 \cos 6\varphi$. The anisotropy energy of such a form derived from a microscopic consideration was used previously to explain the low-field phase transition at $T=0$.⁶ Applying the condition of the lock-in

transition in the single soliton picture (10) to the functional (17) with l and m specified by (16), we obtain the following equation, which defines position of the phase boundary $H_{\text{II-III}}(T)$ between elliptic incommensurate and commensurate phases,

$$H^6 = \frac{(\pi B \beta_2)^2}{2A \gamma \chi_2^2} \left\{ H^2 + \frac{2\beta_2 \chi_3}{\beta_1 \chi_2} [H_c^2(T) - H^2] \right\}. \quad (18)$$

This equation is solved numerically below using estimates for the phenomenological constants. Since at the phase boundary $H_c(T)$ the functional F'' transforms into the corresponding functional of the linear phases (7), the solution of Eq. (18) under additional condition $H = H_c(T)$ coincides with (11). Thus, we conclude that a multicritical point formed by the two second-order transition lines and two lines of the lock-in transitions appears on the H - T diagram of the row model. Strong enough incommensurability can drive the lock-in transitions into the first order, which agrees with the experimental observations for RbMnBr_3 .

For calculation of the $H_{\text{II-III}}(T)$ line we first fit the experimental boundaries $H_N(T)$, $H_{\text{I-IV}}(T)$, and $H_c(T)$ by expressions (8), (11), and (15) and obtain $T_N = 8.52$ K, $\delta T = 0.75$ K, $\chi_1 = 0.04$, $\chi_3 = 0.11$ (susceptibilities are measured in units of α). The multicritical point is situated for this set of constants at $T^* = 7.96$ K, $H^* = 2.23$ T. Then, the only unknown parameter in Eq. (18) is the ratio β_2/β_1 . The choice $\beta_2 = \beta_1$ gives a reasonable behavior of the fourth phase boundary in the vicinity of the multicritical point (Fig. 1).

Since we kept only the leading terms in temperature dependences of critical fields on the small parameter $(1 - T/T_N)$, the presented Landau-type theory accounts well only the region of the phase diagram near T_N . Better agreement at low temperatures may be achieved introducing additional terms into the functional (5), e.g., $(\mathbf{S} \cdot \mathbf{S}^*)^3$ or $H^2 |\mathbf{H} \cdot \mathbf{S}|^2$.^{21,22} We do not apply this procedure because it has, in contrast to our consideration, a large number of adjustable parameters and relative importance of different terms cannot be clarified by comparison to the experiment.

IV. CONCLUSIONS

The phenomenological analysis of ordered spin states of the row model in magnetic field shows an unexpectedly rich phase diagram. This model explains the complicated magnetic diagram of the triangular lattice antiferromagnet RbMnBr_3 with a multicritical point formed by an intersection of two critical lines and two lines of first-order transitions. Two incommensurate phases of RbMnBr_3 having the common wave vector are identified to differ in their polarization: linear at high fields and elliptic at low fields. The commensurate phases of the row model possess the same wave vector as spin states of the fully frustrated antiferromagnet CsMnBr_3 .⁸ Though more complicated Bragg patterns are seen on the experiment^{11,12} (because of the unknown, probably, multidomain structure of the crystal lattice in RbMnBr_3), our analysis suggests that the primary effect on the magnetic phase diagram is from an orthorhombic distortion of exchange bonds. The qualitative role of the magnetic field is to support linear polarization of the order parameter. Therefore, the sixth-order term, which is of the exchange origin, becomes anisotropic in magnetic field and favors commensurate states. However, the lock-in of the wave vectors occurs only at intermediate field region, whereas both low-field and high-field phases are incommensurate. Note that such reentrant appearance of the incommensurate phase should take place even at $T = 0$ near the saturation field. From the discussion of Ref. 27 and the order-parameter analysis given above, it is also evident that the critical behaviors on the second-order transition lines are the same as for CsMnBr_3 . Namely, the $H_N(T)$ boundary is of the XY universality class, while the $H_c(T)$ line corresponds to the Ising-type criticality.

ACKNOWLEDGMENTS

The author thanks O. A. Petrenko for fruitful discussions. He is grateful to B. Lüthi and to the Physikalisches Institut, Universität Frankfurt am Main, where this work was done, for their kind hospitality.

*Present address: Institute for Solid State Physics, University of Tokyo, Tokyo 106, Japan.

¹J. L. Mañes, M. J. Tello, and J. M. Pérez-Mato, *Phys. Rev. B* **26**, 250 (1982); A. Hauser, U. Falk, P. Fischer, and H. U. Güdel, *J. Solid State Chem.* **56**, 343 (1985); A. Harrison and D. Visser, *J. Phys. Condens. Matter* **1**, 733 (1989).

²M. L. Plumer, A. Caillé, and H. Kawamura, *Phys. Rev. B* **44**, 4461 (1991).

³H. Kawamura, *Prog. Theor. Phys. Suppl.* **101**, 545 (1990).

⁴W. Zhang, W. M. Saslow, and M. Gabay, *Phys. Rev. B* **44**, 5129 (1991).

⁵W. Zhang, W. M. Saslow, M. Gabay, and M. Benakli, *Phys. Rev. B* **48**, 10 204 (1993).

⁶M. E. Zhitomirsky, O. A. Petrenko, and L. A. Prozorova, *Phys. Rev. B* **52**, 3511 (1995).

⁷C. J. Glinka, V. J. Minkiewicz, D. E. Cox, and C. P. Khattak, in *Magnetism and Magnetic Materials*, edited by C. D. Graham and J. J. Rhyne, AIP Conf. Proc. No. 10 (AIP, New York, 1973), p. 659.

⁸B. D. Gaulin, T. E. Mason, M. F. Collins, and J. Z. Larese, *Phys. Rev. Lett.* **62**, 1380 (1989).

⁹A. N. Bazhan, I. A. Zaliznyak, D. V. Nikiforov, O. A. Petrenko, S. V. Petrov, and L. A. Prozorova, *Zh. Éksp. Teor. Fiz.* **103**, 691 (1993) [*Sov. Phys. JETP* **76**, 342 (1993)].

¹⁰I. M. Vitebskii, O. A. Petrenko, S. V. Petrov, and L. A. Prozorova, *Zh. Éksp. Teor. Fiz.* **103**, 326 (1993) [*Sov. Phys. JETP* **76**, 178 (1993)].

¹¹T. Kato, T. Ishii, Y. Ajiro, T. Asano, and S. Kawano, *J. Phys. Soc. Jpn.* **62**, 3384 (1993).

¹²L. Heller, M. F. Collins, Y. S. Yang, and B. Collier, *Phys. Rev. B* **49**, 1104 (1994).

¹³T. Kato, T. Asano, Y. Ajiro, S. Kawano, T. Ishii, and K. Iio, *Physica B* **213&214**, 182 (1995).

¹⁴Note, that the fourth phase boundary at low T , high H was not detected in Ref. 12, though its existence is clearly confirmed by magnetization (Refs. 9 and 15) and neutron (Ref. 11) measurements. We, however, keep the corresponding data (Ref. 12) for the rest three boundaries, because they have been determined with a higher accuracy than in other works.

¹⁵T. Asano, Y. Ajiro, M. Mekata, H. A. Katori, and T. Goto, *Physica B* **201**, 75 (1994).

- ¹⁶T. Kato, K. Iio, T. Hoshino, T. Mitsui, and H. Tanaka, *J. Phys. Soc. Jpn.* **61**, 275 (1992).
- ¹⁷E. Rastelli and A. Tassi, *Phys. Rev. B* **52**, 12 755 (1995); *Z. Phys. B* **97**, 147 (1995); **99**, 61 (1995).
- ¹⁸O. A. Petrenko, M. F. Collins, C. V. Stager, B. Collier, and Z. Tun, *J. Appl. Phys.* **79**, 2617 (1996).
- ¹⁹T. Kato, K. Machida, T. Ishii, K. Iio, and T. Mitsui, *Phys. Rev. B* **50**, 13 039 (1994).
- ²⁰M. L. Plumer and A. Caillé, *Phys. Rev. B* **42**, 10 388 (1990).
- ²¹X. Zhu and M. B. Walker, *Phys. Rev. B* **36**, 3830 (1987); M. L. Plumer, K. Hood, and A. Caillé, *Phys. Rev. Lett.* **60**, 45 (1988).
- ²²M. L. Plumer and A. Caillé, *Phys. Rev. B* **41**, 2543 (1990).
- ²³A. V. Chubukov, *J. Phys. C* **21**, L441 (1988).
- ²⁴I. E. Dzyaloshinsky, *Zh. Éksp. Teor. Fiz.* **47**, 992 (1964) [*Sov. Phys. JETP* **20**, 665 (1965)]; P. Bak and V. J. Emery, *Phys. Rev. Lett.* **36**, 978 (1976).
- ²⁵P. Bak, in *Solitons and Condensed Matter Physics*, edited by A. R. Bishop and T. Schneider (Springer, Berlin, 1978), p. 216.
- ²⁶A. E. Jacobs and M. B. Walker, *Phys. Rev. B* **21**, 4132 (1980); P. Prelovšek, *J. Phys. C* **15**, L269 (1982).
- ²⁷H. Kawamura, A. Caillé, and M. L. Plumer, *Phys. Rev. B* **41**, 4416 (1990).